Medicinal Chemistry Research (2022) 31:1916–1930
https://doi.org/10.1007/s00044-022-02947-2

MEDICINAL CHEMISTRY RESEARCH

ORIGINAL RESEARCH

Discovery of novel HCV inhibitors: design, synthesis and biological activity of phthalamide derivatives

Mahdi Mahjoub[1] · Smohammad Mahboubi-Rabbani[1] · Rouhollah Vahabpour[2] · Afshin Zarghi[1] · Elham Rezaee[1] · Sayyed Abbas Tabatabai[1]

Received: 18 May 2022 / Accepted: 6 August 2022 / Published online: 30 August 2022
© The Author(s), under exclusive licence to Springer Science+Business Media, LLC, part of Springer Nature 2022

Abstract

Hepatitis C virus (HCV) is a major cause of end-stage liver diseases like hepatocarcinoma, posing a serious worldwide threat when left untreated. Nowadays, direct-acting antivirals (DAAs) constitute core components of anti-HCV treatment. Nonetheless, some DAAs are associated with a growing level of drug resistance as well as adverse reactions. That is why introducing new anti-HCV drugs with higher potency and lower toxicity is so essential. NS5B polymerase is an HCV non-structural protein acts as a critical target for the development of anti-HCV therapeutics. Based on these essential requirements for the inhibition of HCV NS5B polymerase, a novel series of phthalamide analogs that harbor the potential of NS5B polymerase inhibition to stop HCV proliferation in a cell-based assay were developed. Interestingly, all compounds displayed low cellular cytotoxicity in Huh 7.5 cells ($CC_{50} > 100$) and proper EC_{50} values against HCV replication. Docking studies revealed that compounds with metal coordinating groups may be able to prevent the binding of the natural substrate of NS5B, which is a nucleotide, via binding to the metal cations present in the enzyme. In agreement with the biological studies, most of the designed compounds have considerable affinity to the active site in comparison with sofosbuvir. Compound 3z with EC_{50} of 6.0 µM, and an appropriate affinity to the active site could be considered as a new hit for the design of novel HCV inhibitors.

Graphical abstract

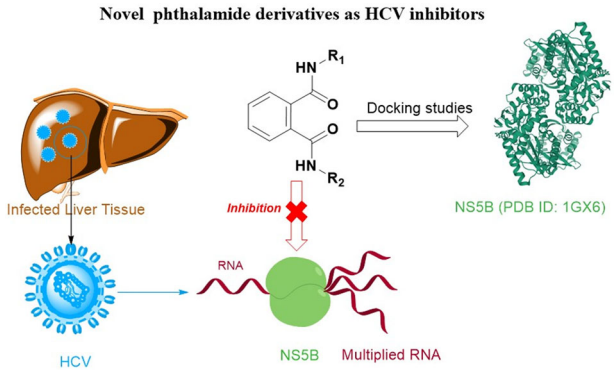

Supplementary information The online version contains supplementary material available at https://doi.org/10.1007/s00044-022-02947-2.

✉ Elham Rezaee
elham_rezaee63@yahoo.com

✉ Sayyed Abbas Tabatabai
sa_tabatabai@yahoo.com

[1] Department of Pharmaceutical Chemistry, School of Pharmacy, Shahid Beheshti University of Medical Sciences, Tehran, Iran

[2] Department of Medical Lab Technology, School of Allied Medical Sciences, Shahid Beheshti University of Medical Sciences, Tehran, Iran

Keywords HCV inhibitors · Docking · Synthesis · Phthalamide · NS5B polymerase

Introduction

Hepatitis C caused by the hepatitis C virus (HCV) is considered globally one of the most severe liver diseases that is a leading cause for hepatocellular carcinoma (HCC) [1, 2]. Based on the reports from the World Health Organization (WHO), nearly a total of 71 million patients is now chronically infected with HCV [3]. Before 2011, the standard of care (SOC) in antiviral therapy for HCV infection was mainly a combination of subcutaneous pegylated interferon-alpha (pegIFN-α) and oral ribavirin which sometimes may cause patients to experience serious adverse reactions [4, 5]. Moreover, no vaccine is yet available for the prevention of HCV [6]. Therefore, there is an unmet clinical need to develop novel chemotherapy against HCV with better efficacy and tolerability. With the discovery of additional direct-acting antiviral agents (DAAs), therapy without using pegIFN-α became possible for curing all HCV genotypes while prominently improving unwanted side effects [7]. DAAs specifically target essential proteins in the HCV life cycle, including NS5B RNA dependent RNA polymerase (RdRp) that plays an essential role in the life cycle of the virus [8, 9]. NS5B is a desirable target for designing new drugs because there is no known NS5B counterpart in the human body [10]. In recent years, a diverse range of small NS5B RdRp molecules have been developed which are classified into the nucleoside inhibitors (NIs), targeting enzyme active site, as well as non-nucleoside inhibitors (NNIs), binding with the allosteric sites known as thumb I, thumb II, palm I, palm II and palm β [11]. At the top of the palm subdomain, the active site of NS5B consists of two divalent ions Mg^{2+} or Mn^{2+} that are coordinated with three conserved aminoacids Asp318, Asp319, and Asp220 [12]. The metal ions play a pivotal role in the catalysis of the phosphodiester bond formation between sequential nucleotides [13]. Therefore, compounds bearing metal coordinating moieties could be utilized for the NS5B inhibition [14]. In general, an aromatic side group is usually connected to the metal-chelating scaffold in the structure of NNIs NS5B inhibitors [10]. Following the initial optimization of aminothiazole 5-carboxylic acid scaffold as NS5B inhibitor, a novel series of 4H-pyrazolo[1,5-α]pyrimidin-7-one analogs were developed by Deng et al. [15]. In this series, the most active compound **A** showed an IC_{50} of 0.05 μM, against HCV genotypes 1–3 along with single digit micromolar inhibition in the HCV replicon assay. Moreover, in 2013, Venkatraman et al. introduced a novel series of tricyclic indole derivatives as NS5B inhibitors, in which "6H-furo[2,3-e]indole-7-carboxylic acid" **B** was identified as the most active molecule with promising cellular activity ($EC_{50} = 160$ nM) and an IC_{50} value of 0.031 μM [16]. Compounds **A** and **B** contain two carbonyl groups that were found to inhibit HCV NS5B [17] (Fig. 1).

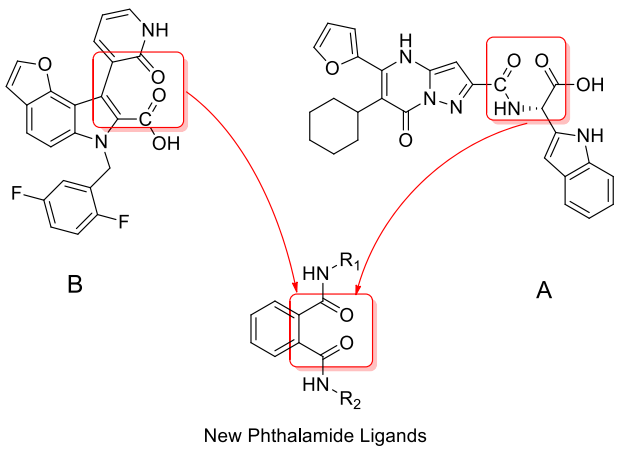

Fig. 1 The logic for designing new phthalamide derivatives as NS5B inhibitors

This structural feature was used in our study to introduce phthalamide derivatives as novel anti-HCV agents targeting NS5B activity. Docking studies demonstrated that these structures had high levels of binding affinity for the NS5B active site. Based on that, the phthalamide scaffold is considered as a core structure substituted with a large number of structurally diverse groups. Since most of the NS5B inhibitors possess two hydrophobic moieties, we put two aralkyl fragments on amide NHs (Fig. 1) and the effect of various substituted aralkyl moieties on HCV inhibition, using a Japonicum Fulminant Hepatitis virus serotype 1 (JFH1)-derived infectious clone was investigated. The phthalamide scaffold was hypothesized to be responsible for insertion into the active site followed by the metal coordination and an aralkyl fragment probably involved in an interaction with hydrophobic aminoacids of the active site.

Results and discussion

Chemistry

Target compounds **3a–3z** were achieved in moderate to high yields (54–99%) by using a convenient two-step procedure starting from phthalic anhydride **1**. As illustrated in Scheme 1, the procedure began with the condensation of phthalic anhydride, with amine derivatives, in ethyl acetate

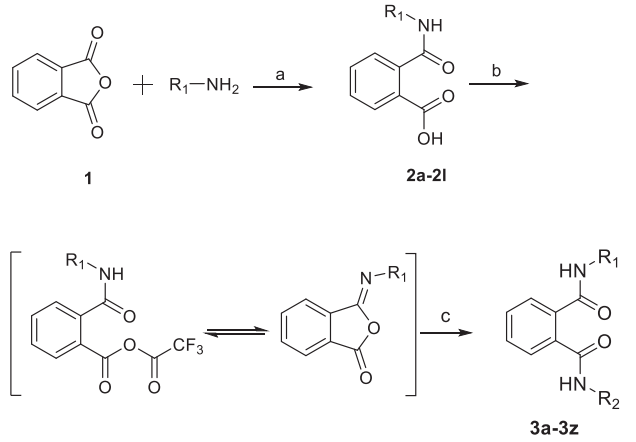

Scheme 1 Reagents and conditions: (**a**) Ethyl acetate, r.t, 18 h; (**b**) Trifluoroacetic anhydride (TFAA), Triethylamine (TEA), THF, 0 °C, 30 min; (**c**) R_2-NH_2, r.t, 24 h

to generate the key intermediates **2a–2l** [18]. The final products **3a–3z** were obtained upon the reaction with trifluoroacetic anhydride, followed by the reaction with differently-substituted primary amines in THF at room temperature [19, 20]. Trifluoroacetic anhydride was used to activate the free carboxyl moiety of the intermediates **2a–2l** by the formation of trifluoroacetic benzoic anhydride followed by isoimide intermediates according to Scheme 1. TEA acts as the base catalyst to deprotonate the free carboxyl, making it ready for reaction with trifluoroacetic acid. The structural characterization of the newly-synthesized analogs was confirmed using elemental analysis and IR, ^{1}H-NMR, ^{13}CNMR, and ESI-MS spectroscopies. Based on the ^{1}H-NMR spectrum, characteristic amide NH signals together with the multiple signals of aromatic ring hydrogens, and the molecular ion signal in the ESI-MS spectrum proved the structure of the synthesized compounds.

HCV replicon assay

Until recent years, it was not possible to detect a whole cycle of HCV replication in cell culture. To study more detailed aspects of HCV reproduction, subgenomic viral RNAs (replicates) able to replicate themselves in human liver cells were developed [21]. In the present study, target compounds **3a–3z** were evaluated in a cell-based viral replication surrogate assay known as the replicon system [22]. The FDA-approved nucleotide polymerase inhibitor, sofosbuvir, was used as a control compound. At the same time, the cell viability was identified using an XTT-based colorimetric assay to ensure that the activity of the molecule is entirely independent of cytotoxic effects. The test also included replicon cells receiving vehicle alone (DMSO) and cell culture medium. EC_{50} and CC_{50} were determined by at least three experiments (Table 1). As clearly shown in Table 1, all phthalamide derivatives demonstrated low cytotoxicity ($CC_{50} > 100$ µM) in Huh-7.5 cells, rendering them viable inhibitors for HCV. Furthermore, most of the target compounds were found active against HCV with the EC_{50} values in the range from 6 to 230 µM. However the newly-developed compounds were found to be less active than the reference sofosbuvir against HCV replication. It may be attributed to the simple structure of the newly-designed structures that prevent them from making more binding interactions. Interestingly, when the N-phenyl is replaced with 2-hydroxyindanyl, the compound 3z becomes a promising HCV inhibitor with an EC_{50} of 6 µM and a decent selectivity ratio, serving as a valuable handle for further structure-activity relationship (SAR) explorations. On the other hand, the substitution of the N-aralkyl moieties with halogens improved antiviral activity as well as cytotoxicity profile. This is exemplified by compounds **3b**, **3d**, **3m**, **3n**, and **3y**, with a fluorine or chlorine substitution at N-phenyl or N-benzyl rings confers relatively acceptable inhibitory activity (11–19 µM). The anti-HCV assay results revealed a few discernible SAR trends. First of all, the substitution of N-aralkyl was found to enhance anti-HCV activity as compounds **3a** and **3x** with unsubstituted benzyl and phenyl, were shown to be approximately inactive ($EC_{50} > 100$ µM). In contrast, most of the analogs with substituted N-aralkyl groups indicated considerable potency. Also, the properties of substituent appeared crucial for inhibitory activity. For instance, the introduction of a hydrophilic substituent like hydroxyl on the appropriate position of the aralkyl moiety was found to significantly influence anti-HCV activity as compound **3z** demonstrated the most anti-HCV activity. Among other molecules, anti-HCV activity increased in the following order: F > Cl > Br > Me > OMe, proposing that substitution with electron-donating groups leads to less active HCV inhibitors. Additionally, it was found that N-substitution with the linear alkyl groups like n-propyl and n-pentyl have a detrimental effect on anti-HCV activity, which may be due to the loss of π interactions between the ligand and the active site. Notably, compound **3p** with cyclohexyl was proven to be considerably less potent ($EC_{50} > 200$ µM) than its aromatic-counterpart **3x** ($EC_{50} = 110$ µM). In monochlorinated analogs **3m** and **3y**, anti-HCV activity was not affected by the position of substituent on the phenyl ring while compound **15** with Cl in meta-position was proven to be less cytotoxic ($EC_{50} = 18$ µM, SI = 18.33) than its para-counterpart 3y ($EC_{50} = 19$ µM, SI = 15.53). In compounds **3f** and **3g** with dimethyl phenyl substitution, changing from 2,3 to 2,6 position increased both the activity ($EC_{50} = 63$ and 55 µM, respectively) and cytotoxicity ($CC_{50} = 430$ and 235 µM, respectively), indicating that the methylation of 6-position is better tolerated by the enzyme active site. As expected, compounds **3b** and **3d** possessing, 4-fluorobenzyl and

Table 1 EC_{50}, CC_{50} & SI for compounds **3a–3z**

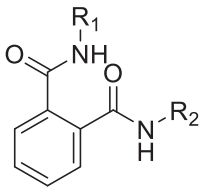

No.	R_1	R_2	EC_{50} (μM)*	CC_{50} (μM)**	SI***	ΔG (kcal/mol)
3a	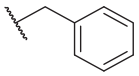	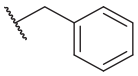	101	650	6.44	−11.22
3b	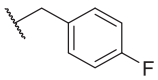	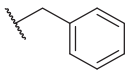	11	385	35.0	−12.31
3c	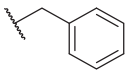	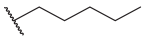	114	420	3.68	−9.66
3d	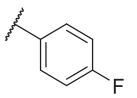	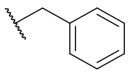	11	346	31.5	−10.13
3e	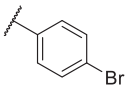	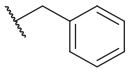	42	165	3.93	−4.20
3f	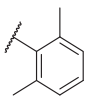	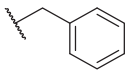	55	235	4.27	−2.15
3g	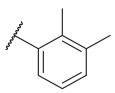	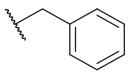	63	430	6.83	−3.75
3h	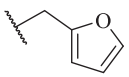	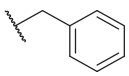	50	385	7.70	−3.32
3i	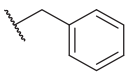	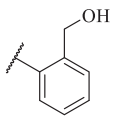	14	380	27.14	−10.22
3j	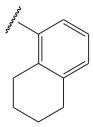	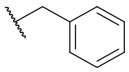	90	245	2.72	−2.98

Table 1 (continued)

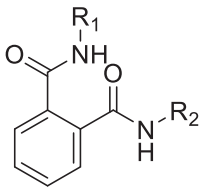

No.	R_1	R_2	EC_{50} (μM)*	CC_{50} (μM)**	SI***	ΔG (kcal/mol)
3k	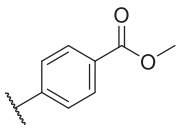	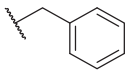	85	185	2.18	−2.22
3l	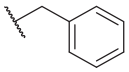	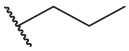	122	430	3.52	−1.11
3m	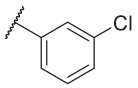	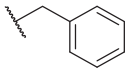	18	330	18.33	−9.21
3n	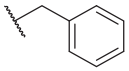	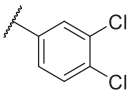	16	205	12.81	−8.12
3o	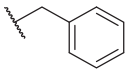	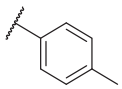	65	460	7.08	−4.52
3p		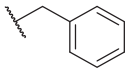	230	430	1.87	−1.04
3q	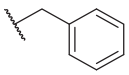	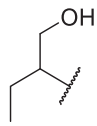	71	155	2.18	−1.31
3r	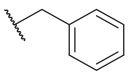	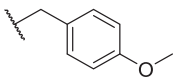	89	335	3.76	−2.22
3s	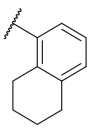	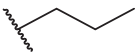	122	451	3.70	−1.56

Table 1 (continued)

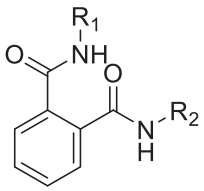

No.	R_1	R_2	EC_{50} (μM)*	CC_{50} (μM)**	SI***	ΔG (kcal/mol)
3t	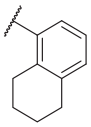	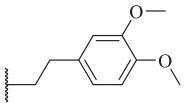	70	350	5.00	−6.10
3u	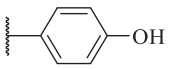	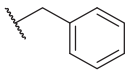	34	110	3.24	−7.34
3v	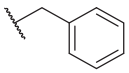	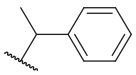	66	220	3.33	−5.22
3w	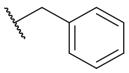	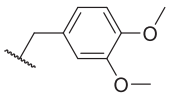	91	220	2.41	−3.15
3x	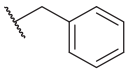	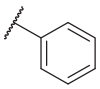	110	245	2.22	−13.52
3y	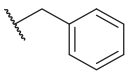	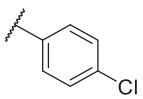	19	295	15.53	−16.34
3z	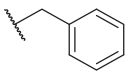	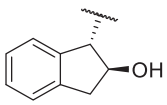	6	476	79.33	−17.13
Sofosbuvir			4	>500	ND****	−22.10

**EC_{50} means the 50% effective concentration;* The lower the EC_{50}, the less the concentration of a drug is required to produce 50% of maximum effect and the higher the potency, vice versa

***CC_{50} means the 50% cytotoxic concentration;* The lower the CC_{50}, the less the concentration of a drug is required to produce 50% of toxic effect and the higher the toxicity; vice versa

****SI (the safety index) was calculated by CC_{50}/EC_{50};*

*****ND* not determined

4-fluorophenyl respectively displayed similar activities with an EC_{50} value of 11 μM. Due to this, a fundamental change in binding mode to the enzyme or the physico-chemical properties can be reflected in the differences in activity and cytotoxicity between substituents and positions, but further research is required to establish detailed structure-activity relationships. In summary, the biological assay of anti-HCV activity showed the phthalamide scaffold could be considered as a promising core to design potent HCV inhibitors.

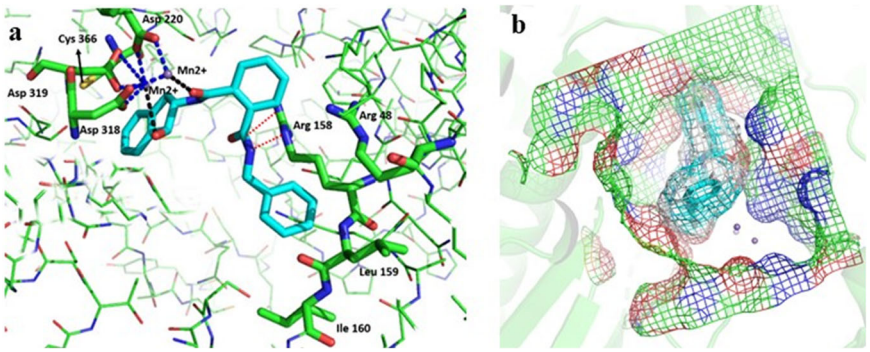

Fig. 2 The minimized docking model of the compound 3z in the NS5B active site. **a** The amide groups of compound 3z interacted with two Mn2+ that are coordinated by active site residues Asp220, Asp318, and Asp319; **b** The surface presentation of ligand-enzyme binding

Molecular modeling studies

The compounds were designed based on the pharmacophore model of NS5B active site inhibitors. Our inhibitors contain a chelating moiety capable of binding to both metal ions at the active site, thus could represent a type of metal-binding NNIs. A five-metal model for NS5B in complex with uridine triphosphate (UTP) (**PDB code: 1GX6**) as a surrogate for the NS5B/viral genome complex, was used in our docking study to explain the molecular recognition interactions. The binding modes of newly-designed compounds within the HCV RdRp catalytic site at the palm domain were computed. According to the docking results and in correlation with biological studies, all compounds showed lower affinity in comparison with sofosbuvir (Table 1). The amide groups of compounds interacted with two Mn^{2+} that are coordinated by active site residues Asp220, Asp318, and Asp319 Compound **3z** was found to fit in the active site perfectly, chelating Mn^{2+} ions of the active site through the carbonyl and hydroxyl groups of phthalamide scaffold with the distances of 2.46 and 2.93 Å (Fig. 2a). The aralkyl moiety of compound **3z** was inserted into a hydrophobic pocket in the enzyme consisting of Leu159 and Ile160, which are essential residues in interaction with the co-crystallized UTP. Besides, the other amide group of phthalamide scaffold formed interactions with the side chain of Arg48 and Arg158, the residues that were observed to form crucial salt bridge interactions with the terminal phosphate of UTP in the original X-ray crystallographic structure. A special hydrophobic bond was also found between the indanol group of compound **3z** and Cys366. In order to validate the docking method, sofosbuvir was docked into the active site of the NS5B; it was found that the used method for docking is valid (Table 1). As shown in Fig. 2b compound 3z fit properly in the active site.

Conclusion

In summary, a novel series of phthalamide analogs were synthesized and evaluated against HCV replication in Huh 7.5 cells. All the newly-synthesized compounds showed reasonable inhibition of the virus multiplication. The outputs of docking analysis was matched with the findings observed experimentally. The results of the investigation demonstrated that compound **3z** bearing the indanol moiety possesses the highest potency as anti-HCV with an EC_{50} of 6 µM and a selectivity ratio of 79.33, which renders this molecule valuable lead scaffold for the development of more potent anti-HCV agents. More in vitro enzyme-specific studies are needed to elucidate the fundamental molecular details of HCV inhibition by these molecules, especially concerning the inhibition of NS5B activity.

Materials and methods

Chemistry

All laboratory-grade chemical reagents and solvents used in this study were obtained commercially from Merck AG or Aldrich Chemical. The reactions were monitored by thin-layer chromatography (TLC) performed on commercially available Merck pre-coated plates (silica gel 60 F254, 0.25 mm), and spots were visualized with UV light. Melting points were determined with an Electrothermal 9100 apparatus and were not corrected. The structures of the newly-synthesized analogs were confirmed by IR, LC-MS, ^{1}HNMR, and ^{13}CNMR spectroscopy methods as well as CHN elemental analysis. Perkin Elmer Model 1420 spectrophotometer, Agilent 6410 triple quadrupole mass spectrometer (LC-MS) with electrospray ionization (ESI) interface, PerkinElmer 843 IR and Costech elemental analyzer (Costech, Italy) were used to obtain Mass spectra, IR, and CHN analysis, respectively. The ^{1}HNMR and ^{13}CNMR spectra were generally acquired in d_6-DMSO solutions on a Bruker spectrometer (Bruker Biosciences, USA), operating at 400 MHz for ^{1}HNMR and 100 MHz for ^{13}CNMR. Chemical shifts are given in ppm relative to the TMS solvent signal. Coupling constant (J) values are estimated in hertz (Hz), and spin multiples

are given as s (singlet), d (doublet), t (triplet), q (quartet), m (multiplet), and br (broad).

Procedure for the synthesis of intermediates 2a–2l

To a mixture of phthalic anhydride in ethyl acetate (1.0 g, 6.8 mmol), various substituted amine derivatives (6.8 mmol) were added. The reaction was stirred at room temperature for 18 h. After completion of the reaction, an equivalent volume of *n*-hexane was added to the mixture, and the precipitated material was filtered off. The residue was washed up by the use of *n*-hexane, diluted aqueous HCl solution, and distilled water to afford the target intermediates **2a–2l**.

2-(benzylcarbamoyl) benzoic acid (2a)

Yield: 97%; MP: 108–111 °C; IR (KBr): 3384 (NH), 2415–3457 (OH), 1677, 1722 (C=O), 1450–1600 (aromatic C-H); LC-MS (ESI) *m/z* 254.1 ($M\text{-}H^+$); Anal. Calcd for $C_{15}H_{13}NO_3$: C, 70.58; H, 5.13; N, 5.49. Found: C, 70.78; H, 5.15; N, 5.47.

2-((4-hydroxyphenyl) carbamoyl) benzoic acid (2b)

Yield: 75%; MP: 135–138 °C; IR (KBr): 3331 (NH), 2357–3543 (OH), 1677, 1734 (C=O), 1450–1600 (aromatic C-H); LC-MS (ESI) *m/z* 256.2 ($M\text{-}H^+$); Anal. Calcd for $C_{14}H_{11}NO_4$: C, 65.37; H, 4.31; N, 5.45. Found: C, 65.32; H, 4.33; N, 5.48.

2-((4-bromophenyl) carbamoyl) benzoic acid (2c)

Yield: 98%; MP: 145–146 °C; IR (KBr): 3377 (NH), 2708–3708 (OH), 1671, 1743 (C=O), 1450–1600 (aromatic C-H); LC-MS (ESI) *m/z* 318.1 ($M\text{-}H^+$), 320.1 ($M+2\text{-}H^+$); Anal. Calcd for $C_{14}H_{10}BrNO_3$: C, 52.52; H, 3.15; N, 4.38. Found: C, 52.49; H, 3.14; N, 4.40.

2-(cyclohexylcarbamoyl) benzoic acid (2d)

Yield: 99%; MP: 154–156 °C; IR (KBr): 3273 (NH), 2663–3390 (OH), 1738 (C=O), 1450–1600 (aromatic C-H); LC-MS (ESI) *m/z* 246.2 ($M\text{-}H^+$); Anal. Calcd for $C_{14}H_{17}NO_3$: C, 68.00; H, 6.93; N, 5.66. Found: C, 67.95; H, 6.95; N, 5.68.

2-((5, 6, 7, 8-tetrahydronaphthalen-1-yl) carbamoyl) benzoic acid (2e)

Yield: 99%; MP: 165–167 °C; IR (KBr): 3310 (NH), 2705–3438 (OH), 1664, 1690 (C=O), 1450–1600 (aromatic C-H); LC-MS (ESI) *m/z* 294.2 ($M\text{-}H^+$); Anal. Calcd for $C_{18}H_{17}NO_3$: C, 73.20; H, 5.80; N, 4.74. Found: C, 73.29; H, 5.77; N, 4.73.

2-((4-fluorophenyl) carbamoyl) benzoic acid (2f)

Yield: 78%; MP: 129–130 °C; IR (KBr): 3317 (NH), 2703–3433 (OH), 1651, 1721 (C=O), 1450–1600 (aromatic C-H); LC-MS (ESI) *m/z* 258.2 ($M\text{-}H^+$); Anal. Calcd for $C_{14}H_{10}FNO_3$: C, 64.87; H, 3.89; N, 5.40. Found: C, 64.81; H, 3.88; N, 5.42.

2-((4-fluorobenzyl) carbamoyl) benzoic acid (2g)

Yield: 73%; MP: 133–134 °C; IR (KBr): 3311 (NH), 2500–3422 (OH), 1647, 1692 (C=O), 1450–1600 (aromatic C-H); LC-MS (ESI) *m/z* 272.2 ($M\text{-}H^+$); Anal. Calcd for $C_{15}H_{12}FNO_3$: C, 65.93; H, 4.43; N, 5.13. Found: C, 65.86; H, 4.42; N, 5.15.

2-((2, 6-dimethylphenyl) carbamoyl) benzoic acid (2h)

Yield: 97%; MP: 136–138 °C; IR (KBr): 3233 (NH), 2398–3363 (OH), 1642, 1703 (C=O), 1450–1600 (aromatic C-H); LC-MS (ESI) *m/z* 268.2 ($M\text{-}H^+$); Anal. Calcd for $C_{16}H_{15}NO_3$: C, 71.36; H, 5.61; N, 5.20. Found: C, 71.25; H, 5.63; N, 5.23.

2-((2, 3-dimethylphenyl) carbamoyl) benzoic acid (2i)

Yield: 99%; MP: 135–137 °C; IR (KBr): 3232 (NH), 2709–3413 (OH), 1632, 1696 (C=O), 1450–1600 (aromatic C-H); LC-MS (ESI) *m/z* 268.2 ($M\text{-}H^+$); Anal. Calcd for $C_{16}H_{15}NO_3$: C, 71.36; H, 5.61; N, 5.20; Found: C, 71.30; H, 5.59; N, 5.22.

2-((furan-2-ylmethyl) carbamoyl) benzoic acid (2j)

Yield: 86%; MP: 125–126 °C; IR (KBr): 3337 (NH), 2468–3462 (OH), 1651, 1693 (C=O), 1450–1600 (aromatic C-H); LC-MS (ESI) *m/z* 244.2 ($M\text{-}H^+$); Anal. Calcd for $C_{13}H_{11}NO_4$: C, 63.67; H, 4.52; N, 5.71; Found: C, 63.57; H, 4.50; N, 5.73.

2-((3-chlorophenyl) carbamoyl) benzoic acid (2k)

Yield: 86%; MP: 122–123 °C; IR (KBr): 3343 (NH), 2553–3435 (OH), 1681, 1736 (C=O), 1450–1600 (aromatic C-H); LC-MS (ESI) *m/z* 274.1 ($M\text{-}H^+$); Anal. Calcd for $C_{14}H_{10}ClNO_3$: C, 60.99; H, 3.66; N, 5.08. Found: C, 60.88; H, 3.66; N, 5.10.

2-((4-(methoxycarbonyl) phenyl) carbamoyl) benzoic acid (2l)

Yield: 86%; MP: 115–116 °C; IR (KBr): 3032 (NH), 2393–3106 (OH), 1695 (C=O), 1450–1600 (aromatic

C-H); LC-MS (ESI) *m/z* 298.2 ($M\text{-}H^+$); Anal. Calcd for $C_{16}H_{13}NO_5$: C, 64.21; H, 4.38; N, 4.68; Found: C, 64.29; H, 4.37; N, 4.69.

Procedure for the synthesis of compounds 3a–3z

The intermediates **2a–2l** (1 mmol) were dissolved in super-dried THF (5 ml), and the solution was cooled to 0 °C. After that, equimolar amounts of trifluoroacetic anhydride (TFAA) and triethylamine (TEA) were added to the mixture. After 30 min of stirring at 0 °C, amine derivatives were added as well. The resulting mixture was allowed to warm to room temperature and stirred for 20 h until the reaction has been completed. Distilled water (5 ml) and ice were added to the mixture, and the obtained precipitate was filtered off. The solid residue was washed up by distilled water and recrystallized from mixture of ethanol and water to afford the final compounds **3a–3z**.

N^1, N^2- dibenzyl phthalamide (3a)

Yield: 95%; MP: 174–175 °C; IR (KBr): 3249, 3309 (NH), 1643 (C=O), 1450–1600 (aromatic C-H); ^{1}H-NMR (d_6-DMSO, 400 MHz) δ ppm, 4.48 (s, 4H, CH_2-N), 7.28–7.31 (t, 2H, N-benzyl (*p*), $J = 8$ Hz), 7.36–7.44 (m, 8H, N-benzyl (*o*, *m*)), 7.54–7.60 (m, 4H, phenylene $H_2/H_3/H_4/H_5$), 8.90 (s, 2H, NH); ^{13}C-NMR (d_6-DMSO, 100 MHz) δ ppm 42.90, 127.14, 127.35, 127.65, 128.14, 128.69, 129.87, 136.82, 139.97, 168.68; LC-MS (ESI) *m/z* 343.2 ($M\text{-}H^+$); Anal. Calcd for $C_{22}H_{20}N_2O_2$: C, 76.72; H, 5.85; N, 8.13. Found: C, 76.65; H, 5.84; N, 8.17.

N^1-(4-fluorobenzyl)-N^2-benzylphthalamide (3b)

Yield: 95%; MP: 175–177 °C; IR (KBr): 3257 (NH), 1633 (C=O), 1450–1600 (aromatic C-H); ^{1}H-NMR (d_6-DMSO, 400 MHz) δ ppm, 4.39–4.43 (m, 4H, CH_2-N), 7.11–7.16 (t, 2H, N-benzyl (*m*), $J = 8$ Hz), 7.24–7.28 (t, 1H, N-benzyl (*p*), $J = 8$ Hz), 7.30–7.43 (m, 6H, 4-fluorobenzyl $H_2/H_3/H_5/H_6$ & N-benzyl (*o*)), 7.51–7.53 (m, 4H, phenylene $H_2/H_3/H_4/H_5$), 8.83–8.86 (m, 2H, NH); ^{13}C-NMR (d_6-DMSO, 100 MHz) δ ppm 42.22, 42.90, 127.63, 128.11, 128.68, 129.57, 129.65, 129.88, 130.27, 130.65, 130.74, 136.11, 136.14, 136.25, 136.76, 136.82, 168.64, 168.73; LC-MS (ESI) *m/z* 361.2 ($M\text{-}H^+$); Anal. Calcd for $C_{22}H_{19}FN_2O_2$: C, 72.91; H, 5.28; N, 7.73. Found: C, 72.85; H, 5.29; N, 7.76.

N^1-benzyl-N^2-pentylphthalamide (3c)

Yield: 65%; MP: 173–174 °C; IR (KBr): 3245 (NH), 1629, 1653 (C=O), 1450–1600 (aromatic C-H); ^{1}H-NMR (d_6-DMSO, 400 MHz) δ ppm, 0.86–0.89 (t, 3H, CH_3, $J = 8$ Hz), 1.27–1.30 (m, 4H, -CH_2-CH_2-), 1.43–1.48 (q, 2H, CH_2-N, $J = 8$, 4 Hz), 3.13–3.18 (q, 2H, CH_2-N, $J = 8$, 4 Hz), 4.42–4.44 (d, 2H, CH_2-N, $J = 8$ Hz), 7.23–7.26 (t, 1H, N-benzyl (*p*), $J = 8$ Hz), 7.31–7.38 (m, 4H, N-benzyl (*o*, *m*)), 7.44–7.50 (m, 4H, phenylene $H_2/H_3/H_4/H_5$), 8.23–8.26 (t, 1H, NH, $J = 8$ Hz), 8.78–8.81 (t, 1H, NH, $J = 8$ Hz); ^{13}C-NMR (d_6-DMSO, 100 MHz) δ ppm 14.39, 22.36, 29.08, 29.22, 119.92, 123.73, 127.96, 128.17, 129.02, 129.89, 129.92, 136.72, 137.37, 140.00, 167.59, 168.07; LC-MS (ESI) *m/z* 323.2 ($M\text{-}H^+$); Anal. Calcd for $C_{20}H_{24}N_2O_2$: C, 74.05; H, 7.46; N, 8.63. Found: C, 74.11; H, 7.44; N, 8.66.

N^1-benzyl-N^2-(4-fluorophenyl) phthalamide (3d)

Yield: 75%; MP: 164 °C; IR (KBr): 3230, 3250 (NH), 1638, 1652 (C=O), 1450–1600 (aromatic C-H); ^{1}H-NMR (d_6-DMSO, 400 MHz) δ ppm, 4.42–4.43 (d, 2H, CH_2-N, $J = 4$ Hz), 7.28–7.43 (m, 7H, N-benzyl (*o, m, p*) & 4-fluorophenyl H_2/H_6), 7.53–7.63 (m, 4H, phenylene H_3/H_4 & 4-fluorophenyl H_3/H_5), 7.71–7.74 (m, 2H, phenylene H_2/H_5), 8.93–8.96 (t, 1H, NH, $J = 8$ Hz), 10.41 (s, 1H, NH); ^{13}C-NMR (d_6-DMSO, 100 MHz) δ ppm 42.79, 127.11, 127.57, 127.65, 128.07, 128.20, 128.63, 128.99, 129.13, 129.31, 129.98, 130.18, 136.30, 136.41, 136.43, 167.55, 168.18; LC-MS (ESI) *m/z* 347.2 ($M\text{-}H^+$); Anal. Calcd for $C_{21}H_{17}FN_2O_2$: C, 72.40; H, 4.92; N, 8.04. Found: C, 72.55; H, 4.90; N, 8.00.

N^1-benzyl-N^2-(4-bromophenyl) phthalamide (3e)

Yield: 95%; MP: 221–223 °C; IR (KBr): 3293 (NH), 1658 (C=O), 1450–1600 (aromatic C-H); ^{1}H-NMR (d_6-DMSO, 400 MHz) δ ppm, 4.42–4.44 (d, 2H, CH_2-N, $J = 8$ Hz), 7.21–7.25 (t, 1H, N- benzyl (*p*), $J = 8$ Hz), 7.28–7.36 (m, 4H, N-benzyl (*o*, *m*)), 7.51–7.70 (m, 8H, 4-bromophenyl $H_2/H_3/H_5/H_6$ & phenylene $H_2/H_3/H_5/H_6$), 8.95–8.98 (t, 1H, NH, $J = 8$ Hz), 10.50 (s, 1H, NH); ^{13}C-NMR (d_6-DMSO, 100 MHz) δ ppm 42.93, 122.03, 127.13, 127.57, 128.07, 128.22, 128.65, 130.07, 130.25, 130.43, 131.89, 136.24, 137.44, 139.19, 139.40, 167.82, 168.09; LC-MS (ESI) *m/z* 407.2 ($M\text{-}H^+$), 409 ($M+2\text{-}H^+$); Anal. Calcd for $C_{21}H_{17}BrN_2O_2$: C, 61.63; H, 4.19; N, 6.84. Found: C, 61.58; H, 4.21; N, 6.86.

N^1-benzyl-N^2-(2, 6-dimethylphenyl) phthalamide (3f)

Yield: 99%; MP: 194–195 °C; IR (KBr): 3277 (NH), 1648, 1671 (C=O), 1450–1600 (aromatic C-H); ^{1}H-NMR (d_6-DMSO, 400 MHz) δ ppm, 2.27 (s, 6H, CH_3), 4.43–4.45 (d, 2H, CH_2-N, $J = 8$ Hz), 7.07–7.12 (m, 3H, 2,6-dimethyl-benzyl $H_3/H_4/H_5$), 7.21–7.24 (t, 1H, N-benzyl (*p*), $J = 8$ Hz), 7.28–7.32 (t, 2H, N-benzyl (*m*), $J = 8$ Hz), 7.36–7.38 (d, 2H, N-benzyl (*o*), $J = 8$ Hz), 7.53–7.60 (m,

3H, phenylene $H_3/H_4/H_5$), 7.69–7.71 (d, 1H, phenylene H_2, $J = 8$ Hz), 8.90–8.93 (t, 1H, NH, $J = 8$ Hz), 9.73 (s, 1H, NH); ^{13}C-NMR (d_6-DMSO, 100 MHz) δ ppm 18.73, 42.87, 126.99, 127.12, 127.60, 128.10, 128.20, 128.25, 128.66, 128.91, 129.06, 129.41, 129.93, 129.98, 134.56, 135.58, 167.25, 168.56; LC-MS (ESI) *m/z* 357.3 (M-H^+); Anal. Calcd for $C_{23}H_{22}N_2O_2$: C, 77.07; H, 6.19; N, 7.82. Found: C, 77.14; H, 6.21; N, 7.79.

N^1-benzyl-N^2-(2, 3-dimethylphenyl) phthalamide (3g)

Yield: 98%; MP: 193 °C; IR (KBr): 3285, 3309 (NH), 1638, 1665 (C=O), 1450–1600 (aromatic C-H); ^{1}H-NMR (d_6-DMSO, 400 MHz) δ ppm, 2.12 (s, 3H, CH_3), 2.24 (s, 3H, CH_3), 4.42–4.43 (d, 2H, CH_2-N, $J = 4$ Hz), 7.01–7.64 (m, 12H, 2,3-dimethylphenyl $H_4/H_5/H_6$ & N-benzyl (*o*, *m*, *p*) & phenylene $H_2/H_3/H_4/H_5$), 8.88–8.91 (t, 1H, NH, $J = 8$ Hz), 9.78 (s, 1H, NH); ^{13}C-NMR (d_6-DMSO, 100 MHz) δ ppm 14.56, 20.65, 42.74, 124.64, 125.53, 127.13, 127.59, 127.63, 128.09, 128.31, 128.65, 129.11, 129.34, 129.87, 130.07, 132.54, 136.52, 136.66, 137.29, 167.71, 168.48; LC-MS (ESI) *m/z* 357.3 (M-H^+); Anal. Calcd for $C_{23}H_{22}N_2O_2$: C, 77.07; H, 6.19; N, 7.82. Found: C, 77.21; H, 6.18; N, 7.80.

N^1-benzyl-N^2-((furan-2-yl) methyl) phthalamide (3h)

Yield: 97%; MP: 175–176 °C; IR (KBr): 3278 (NH), 1644 (C=O), 1450–1600 (aromatic C-H); ^{1}H-NMR (d_6-DMSO, 400 MHz) δ ppm, 4.37–4.42 (m, 4H, CH_2-N), 6.34–6.39 (m, 2H, furfuryl H_3/H_5), 7.21–7.24 (t, 1H, N-benzyl (*p*), $J = 8$ Hz), 7.29–7.37 (m, 4H, N-benzyl (*o, m*)), 7.47–7.56 (m, 5H, furfuryl H_4 & phenylene $H_2/H_3/H_4/H_5$), 8.76–8.82 (m, 2H, NHs); ^{13}C-NMR (d_6-DMSO, 100 MHz) δ ppm 36.64, 42.94, 107.16, 111.02, 127.16, 127.67, 128.14, 128.24, 128.71, 129.35, 129.87, 129.96, 136.53, 136.80, 139.96, 142.40, 168.56, 168.65; LC-MS (ESI) *m/z* 333.2 (M-H^+); Anal. Calcd for $C_{20}H_{18}N_2O_3$: C, 71.84; H, 5.43; N, 8.38. Found: C, 71.78; H, 5.42; N, 8.40.

N^1-benzyl-N^2-(2-(hydroxymethyl) phenyl) phthalamide (3i)

Yield: 68%; MP: 155–157 °C; IR (KBr): 3350 (NH), 3050–3400 (OH), 1678 (C=O), 1450–1600 (aromatic C-H); ^{1}H-NMR (d_6-DMSO, 400 MHz) δ ppm, 4.45–4.46 (d, 2H, CH_2-N, $J = 4$ Hz), 4.61–4.62 (d, 2H, CH_2-O, $J = 4$ Hz), 5.36–5.39 (t, 1H, OH, $J = 8$ Hz), 7.17–7.25 (m, 2H, N-benzyl (*p*) & 2-aminobenzylalcohol H_6), 7.28–7.31 (m, 3H, N-benzyl (*m*) & 2- aminobenzylalcohol H_4), 7.36–7.38 (d, 2H, N-benzyl (*o*), $J = 8$ Hz), 7.41–7.43 (d, 1H, 2-aminobenzylalcohol H_5, $J = 8$ Hz), 7.57–7.63 (m, 3H, phenylene H_3/H_4 & 2-aminobenzylalcohol H_3), 7.66–7.69 (m, 2H, phenylene H_2/H_5), 8.96–8.99 (t, 1H, NH, $J = 8$ Hz), 9.80 (s, 1H, NH); ^{13}C-NMR (d_6-DMSO, 100 MHz) δ ppm 42.94, 60.96, 124.50, 125.25, 127.14, 127.46, 127.62, 127.79, 128.01, 128.23, 128.66, 129.86, 130.15, 130.25, 135.35, 136.22, 136.54, 137.26, 167.41, 168.36; LC-MS (ESI) *m/z* 359 (M-H^+); Anal. Calcd for $C_{22}H_{20}N_2O_3$: C, 73.32; H, 5.59; N, 7.77; Found: C, 73.44; H, 5.61; N, 7.74.

N^1-benzyl-N^2-(1, 2, 3, 4-tetrahydronaphthalen-8-yl) phthalamide (3j)

Yield: 99%; MP: 220–222 °C; IR (KBr): 3263, 3294 (NHs), 1628, 1657 (C=O), 1450–1600 (aromatic C-H); ^{1}H-NMR (d_6-DMSO, 400 MHz) δ ppm, 1.69 (m, 4H, CH_2-CH_2), 2.69–2.74 (m, 4H, 2 CH_2), 4.44–4.45 (d, 2H, CH_2-N, $J = 4$ Hz), 6.93–6.95 (d, 1H, tetrahydronaphthylamine H_4, $J = 8$ Hz), 7.07–7.10 (t, 1H, tetrahydronaphthylamine H_3, $J = 8$ Hz), 7.21–7.29 (m, 4H, N- benzyl (*m*, *p*) & tetrahydronaphthylamine H_2), 7.34–7.36 (d, 2H, N-benzyl (*o*), $J = 8$ Hz), 7.54–7.65 (m, 4H, phenylene $H_2/H_3/H_4/H_5$), 8.90–8.93 (t, 1H, NH, $J = 8$ Hz), 9.60 (s, 1H, NH); ^{13}C-NMR (d_6-DMSO, 100 MHz) δ ppm 22.86, 22.95, 24.62, 29.71, 42.94, 123.85, 125.40, 126.80, 127.13, 127.60, 128.09, 128.38, 128.65, 129.90, 130.08, 132.30, 136.45, 137.39, 137.78, 139.88, 167.61, 168.49; LC-MS (ESI) *m/z* 383.2 (M-H^+); Anal. Calcd for $C_{25}H_{24}N_2O_2$: C, 78.10; H, 6.29; N, 7.29. Found: C, 78.33; H, 6.28; N, 7.25.

Methyl 4-(2-(benzylcarbamoyl) benzamido) benzoate (3k)

Yield: 70%; MP: 170–171 °C; IR (KBr): 3033, 3290 (NHs), 1630, 1657 (C=O), 1450–1600 (aromatic C-H); ^{1}H-NMR (d_6-DMSO, 400 MHz) δ ppm, 3.83 (s, 3H, OCH_3), 4.43–4.44 (d, 2H, CH_2-N, $J = 4$ Hz), 7.20–7.47 (m, 5H, N-benzyl (*o*, *m*, *p*)), 7.55–7.67 (m, 4H, phenylene $H_2/H_3/H_4/H_5$), 7.86–7.88 (d, 2H, methyl benzoate H_2/H_6, $J = 8$ Hz), 7.94–7.96 (d, 2H, methyl benzoate H_3/H_5, $J = 8$ Hz), 9.02–9.05 (t, 1H, NH, $J = 8$ Hz), 10.75 (s, 1H, NH); ^{13}C-NMR (d_6-DMSO, 100 MHz) δ ppm 42.97, 52.35, 128.07, 128.26, 128.64, 128.92, 129.08, 129.32, 129.85, 130.14, 130.30, 130.63, 134.54, 135.05, 136.15, 137.39, 166.37, 168.00, 168.24; LC-MS (ESI) *m/z* 387.2 (M-H^+); Anal. Calcd for $C_{23}H_{20}N_2O_4$: C, 71.12; H, 5.19; N, 7.21. Found: C, 71.39; H, 5.17; N, 7.23.

N^1-benzyl-N^2-propylphthalamide (3l)

Yield: 91%; MP: 160 °C; IR (KBr): 3150–3335 (NHs), 1623 (C=O), 1450–1600 (aromatic C-H); ^{1}H-NMR (d_6-DMSO, 400 MHz) δ ppm, 0.87–0.90 (t, 3H, CH_3, $J = 8$ Hz), 1.44–1.50 (q, 2H, CH_2, $J = 8$ Hz), 3.10–3.15 (q, 2H, CH_2-N, $J = 8$ Hz), 4.41–4.43 (d, 2H, CH_2-N, $J = 8$ Hz), 7.22–7.26 (t, 1H, N-benzyl (*p*), $J = 8$ Hz), 7.31–7.38 (m, 4H, N-benzyl (*o*, *m*)), 7.43–7.51 (m, 4H, phenylene H_2/H_3/

H_4/H_5), 8.24–8.27 (t, 1H, NH, $J = 8$ Hz), 8.77–8.80 (t, 1H, NH, $J = 8$ Hz); ^{13}C-NMR (d_6-DMSO, 100 MHz) δ ppm 11.95, 22.73, 41.33, 42.89, 127.13, 127.63, 128.11, 128.66, 129.66, 129.82, 136.53, 137.12, 139.95, 168.57, 168.66; LC-MS (ESI) *m/z* 295.0 (M-H$^+$); Anal. Calcd for $C_{18}H_{20}N_2O_2$: C, 72.95; H, 6.80; N, 9.45. Found: C, 72.67; H, 6.76; N, 9.40.

N^1-benzyl-N^2-(3-chlorophenyl) phthalamide (3m)

Yield: 89%; MP: 172–173 °C; IR (KBr): 3287, 3322 (NHs), 1658, 1679 (C=O), 1450–1600 (aromatic C-H); ^{1}H-NMR (d_6-DMSO, 400 MHz) δ ppm, 4.42–4.43 (d, 2H, CH_2-N, $J = 4$ Hz), 7.11–7.37 (m, 7H, N-benzyl (*o, m, p*) & 3-chlorophenyl H_5/H_6), 7.55–7.65 (m, 5H, 3-chlorophenyl H_4 & phenylene $H_2/H_3/H_4/H_5$), 7.93 (s, 1H, 3-chlorophenyl H_2), 8.95–8.98 (t, 1H, NH, $J = 8$ Hz), 10.54 (s, 1H, NH); ^{13}C-NMR (d_6-DMSO, 100 MHz) δ ppm 42.96, 118.33, 119.39, 123.44, 127.14, 127.58, 128.08, 128.63, 130.13, 130.30, 130.79, 133.46, 136.18, 137.36, 139.88, 141.45, 168.04; LC-MS (ESI) *m/z* 363.2 (M-H$^+$); Anal. Calcd for $C_{21}H_{17}ClN_2O_2$: C, 69.14; H, 4.70; N, 7.68. Found: C, 69.23; H, 4.71; N, 7.65.

N^1-benzyl-N^2-(3, 4-dichlorophenyl) phthalamide (3n)

Yield: 97%; MP: 178–179 °C; IR (KBr): 3257, 3273 (NHs), 1641, 1662 (C = O), 1450–1600 (aromatic C-H); ^{1}H-NMR (d_6-DMSO, 400 MHz) δ ppm, 4.42–4.43 (d, 2H, CH_2-N, $J = 4$ Hz), 7.20–7.35 (m, 5H, N-benzyl (*o, m, p*)), 7.55–7.66 (m, 6H, 3,4-dichlorophenyl H_5/H_6 & phenylene $H_2/H_3/H_4/H_5$), 8.10 (s, 1H, 3,4-dichlorophenyl H_2), 8.97–9.00 (t, 1H, NH, $J = 8$ Hz), 10.64 (s, 1H, NH); ^{13}C-NMR (d_6-DMSO, 100 MHz) δ ppm 41.86, 124.04, 126.04, 126.48, 126.56, 127.00, 127.08, 127.30, 127.53, 129.14, 129.26, 129.95, 130.27, 135.02, 136.08, 138.76, 138.99, 166.81, 167.03; LC-MS (ESI) *m/z* 397.2 (M-H$^+$); Anal. Calcd for $C_{21}H_{16}Cl_2N_2O_2$: C, 63.17; H, 4.04; N, 7.02. Found: C, 63.22; H, 4.03; N, 6.98.

N^1-benzyl-N^2-p-tolylphthalamide (3o)

Yield: 99%; MP: 175–176 °C; IR (KBr): 3152–3360 (NHs), 1643 (C=O), 1450–1600 (aromatic C-H); ^{1}H-NMR (d_6-DMSO, 400 MHz) δ ppm, 2.28 (s, 3H, CH_3), 4.42–4.44 (d, 2H, CH_2-N, $J = 8$ Hz), 7.13–7.15 (d, 2H, 4-tolyl H_3/H_5, $J = 8$ Hz), 7.21–7.24 (t, 1H, N-benzyl (*p*), $J = 8$ Hz), 7.27-7.31 (t, 2H, N-benzyl (*m*), $J = 8$ Hz), 7.35–7.37 (d, 2H, N-benzyl (o), $J = 8$ Hz), 7.53–7.61 (m, 6H, 4-tolyl H_2/H_6 & phenylene $H_2/H_3/H_4/H_5$), 8.91–8.94 (t, 1H, NH, $J = 8$ Hz), 10.27 (s, 1H, NH); ^{13}C-NMR (d_6-DMSO, 100 MHz) δ ppm; 20.99, 42.91, 119.98, 127.11, 127.58, 128.06, 128.24, 128.64, 129.41, 129.89, 130.10, 132.61, 136.40, 137.54, 137.63, 139.91, 167.38, 168.31; LC-MS (ESI) *m/z* 343.3 (M-H$^+$); Anal. Calcd for $C_{22}H_{20}N_2O_2$: C, 76.72; H, 5.85; N, 8.13. Found: C, 76.65; H, 5.84; N, 8.11.

N^1-benzyl-N^2-cyclohexylphthalamide (3p)

Yield: 95%; MP: 175–176 °C; IR (KBr): 3259, 3320 (NHs), 1643, 1675 (C=O), 1450–1600 (aromatic C-H); ^{1}H-NMR (d_6-DMSO, 400 MHz) δ ppm, 1.08–1.77 (m, 10H, cyclohexyl $H_2/H_{2'}/H_3/H_{3'}/H_4/H_{4'}/H_5/H_{5'}/H_6/H_{6'}$), 3.59–3.65 (m, 1H, cyclohexyl H_1), 4.41–4.42 (d, 2H, CH_2-N, $J = 4$ Hz), 7.21–7.24 (t, 1H, N-benzyl (*p*), $J = 8$ Hz), 7.29–7.36 (m, 4H, N-benzyl (*o, m*)), 7.41–7.50 (m, 4H, phenylene $H_2/H_3/H_4/H_5$), 8.09–8.11 (d, 1H, NH, $J = 8$ Hz), 8.74–8.77 (t, 1H, NH, $J = 8$ Hz); ^{13}C-NMR (d_6-DMSO, 100 MHz) δ ppm; 25.15, 25.72, 32.65, 42.91, 48.53, 127.16, 127.65, 128.08, 128.26, 128.66, 129.60, 129.82, 136.33, 137.14, 139.89, 167.77, 168.67; LC-MS (ESI) *m/z* 335.3 (M-H$^+$); Anal. Calcd for $C_{21}H_{24}N_2O_2$: C, 74.97; H, 7.19; N, 8.33. Found: C, 74.89; H, 7.21; N, 8.37.

N^1-benzyl-N^2-(1-hydroxybutan-2-yl) phthalamide (3q)

Yield: 67%; MP: 136–137 °C; IR (KBr): 2903–3357 (NHs & OH), 1668, 1681 (C=O), 1450–1600 (aromatic C-H); ^{1}H-NMR (d_6-DMSO, 400 MHz) δ ppm, 0.88–0.91 (t, 3H, CH_3, $J = 8$ Hz), 1.33–1.64 (m, 2H, CH_2), 2.49 (s, 1H, OH), 3.31–3.46 (m, 2H, CH_2-O), 3.75–3.78 (m, 1H, CH-N), 4.42–4.44 (d, 2H, CH_2-N, $J = 8$ Hz), 7.22–7.25 (t, 1H, N-benzyl (*p*), $J = 8$ Hz), 7.30–7.38 (m, 4H, N-benzyl (*o, m*)), 7.48–7.54 (m, 4H, phenylene $H_2/H_3/H_4/H_5$), 7.96–7.98 (d, 1H, NH, $J = 8$ Hz), 8.84–8.87 (t, 1H, NH, $J = 8$ Hz); ^{13}C-NMR (d_6-DMSO, 100 MHz) δ ppm; 10.24, 24.06, 42.97, 53.38, 63.55, 127.15, 127.64, 127.86, 128.11, 128.24, 128.68, 129.07, 129.59, 129.93, 136.07, 137.43, 139.84, 168.66, 168.79; LC-MS (ESI) *m/z* 325.0 (M-H$^+$); Anal. Calcd for $C_{19}H_{22}N_2O_3$: C, 69.92; H, 6.79; N, 8.58. Found: C, 69.88; H, 6.81; N, 8.60.

N^1-(4-methoxybenzyl)-N^2-benzylphthalamide (3r)

Yield: 85%; MP: 174–175 °C; IR (KBr): 3313, 3351 (NHs), 1665, 1695 (C=O), 1450–1600 (aromatic C-H); ^{1}H-NMR (d_6-DMSO, 400 MHz) δ ppm, 3.72 (s, 3H, OCH_3), 4.33–4.35 (d, 2H, CH_2-N, $J = 8$ Hz), 4.41–4.43 (d, 2H, CH_2-N, $J = 8$ Hz), 6.86–6.88 (d, 2H, 4-methoxybenzyl H_3/H_5, $J = 8$ Hz), 7.22–7.38 (m, 7H, 4-methoxybenzyl H_2/H_6 & N-benzyl (*o*, *m*, *p*)), 7.48–7.52 (m, 4H, phenylene $H_2/H_3/H_4/H_5$), 8.74–8.77 (t, 1H, NH, $J = 8$ Hz), 8.80–8.83 (t, 1H, NH, $J = 8$ Hz); ^{13}C-NMR (d_6-DMSO, 100 MHz) δ ppm; 42.38, 42.90, 55.50, 127.12, 127.64, 128.12, 128.67, 128.98, 129.81, 131.85, 136.77, 136.83, 139.95, 158.60, 168.52, 168.68; LC-MS (ESI) *m/z* 373.2 (M-H$^+$); Anal.

Calcd for $C_{23}H_{22}N_2O_3$: C, 73.78; H, 5.92; N, 7.48. Found: C, 73.68; H, 5.90; N, 7.49.

N^1-propyl-N^2-(5, 6, 7, 8-tetrahydronaphthalen-1-yl) phthalamide (3s)

Yield: 98%; MP: 186 °C; IR (KBr): 3310 (NHs), 1655, 1674 (C=O), 1450–1600 (aromatic C-H); ^{1}H-NMR (d_6-DMSO, 400 MHz) δ ppm, 0.86–0.90 (t, 3H, CH_3, $J = 8$ Hz), 1.46–1.52 (q, 2H, CH_2, $J = 8$ Hz), 1.70–1.72 (m, 4H, tetrahydronaphthyl H_6/$H_{6'}$/H_7/$H_{7'}$), 2.69–2.74 (m, 4H, tetrahydronaphthyl H_5/$H_{5'}$/H_8/$H_{8'}$), 3.13–3.17 (q, 2H, CH_2-N, $J = 8$, 4 Hz), 6.92–6.94 (d, 1H, tetrahydronaphthyl H_4, $J = 8$ Hz), 7.07–7.10 (t, 1H, tetrahydronaphthyl H_3, $J = 8$, 4 Hz), 7.26- 7.28 (d, 1H, tetrahydronaphthyl H_2, $J = 8$ Hz), 7.51–7.62 (m, 4H, phenylene H_2/H_3/H_4/H_5), 8.34–8.37 (t, 1H, NH, $J = 8$ Hz), 9.56 (s, 1H, NH); ^{13}C-NMR (d_6-DMSO, 100 MHz) δ ppm; 11.93, 22.77, 22.87, 22.97, 24.60, 29.70, 41.37, 123.74, 125.40, 126.78, 128.01, 128.35, 129.85, 132.22, 136.47, 136.81, 137.14, 137.76, 167.56, 168.40; LC-MS (ESI) *m/z* 335.3 (M-H$^+$); Anal. Calcd for $C_{21}H_{24}N_2O_2$: C, 74.97; H, 7.19; N, 8.33. Found: C, 74.87; H, 7.20; N, 8.30.

N^1-(3, 4-dimethoxyphenethyl)-N^2-(5, 6, 7, 8-tetrahydronaphthalen-1-yl) phthalamide (3t)

Yield: 83%; MP: 172–173 °C; IR (KBr): 3300, 3332 (NHs), 1654, 1683 (C=O), 1450–1600 (aromatic C-H); ^{1}H-NMR (d_6-DMSO, 400 MHz) δ ppm, 1.71–1.72 (m, 4H, tetrahydronaphthyl H_6/$H_{6'}$/H_7/$H_{7'}$), 2.72–2.76 (m, 6H, tetrahydronaphthyl H_5/$H_{5'}$/H_8/$H_{8'}$ & CH_2), 3.37–3.42 (q, 2H, CH_2-N, $J = 8$ Hz), 3.70 (s, 3H, OCH_3), 3.72 (s, 3H, OCH_3), 6.74–6.76 (d, 1H, tetrahydronaphthyl H_4, $J = 8$ Hz), 6.84–6.86 (m, 2H, dimethoxyphenethyl H_2 & tetrahydronaphthyl H_2), 6.93–6.95 (d, 1H, dimethoxyphenethyl H_6, $J = 8$ Hz), 7.08–7.11 (t, 1H, tetrahydronaphthyl H_3, $J = 8$. 4 Hz), 7.27–7.29 (d, 1H, dimethoxyphenethyl H_5, $J = 8$ Hz), 7.46–7.55 (m, 3H, phenylene H_3/H_4/H_5), 7.62–7.64 (d, 1H, phenylene H_2, $J = 8$ Hz), 8.42–8.45 (t, 1H, NH, $J = 8$ Hz), 9.59 (s, 1H, NH); ^{13}C-NMR (d_6-DMSO, 100 MHz) δ ppm; 22.99, 24.64, 29.70, 33.62, 34.97, 41.50, 55.69, 55.78, 120.92, 121.03, 123.49, 123.79, 125.42, 126.81, 127.97, 128.38, 129.83, 129.94, 131.00, 131.96, 132.27, 132.43, 136.49, 136.71, 137.23, 137.79, 168.18, 168.40; LC-MS (ESI) *m/z* 457.4 (M-H$^+$); Anal. Calcd for $C_{28}H_{30}N_2O_4$: C, 73.34; H, 6.59; N, 6.11. Found: C, 73.24; H, 6.57; N, 6.09.

N^1-benzyl-N^2-(4-hydroxyphenyl) phthalamide (3u)

Yield: 68%; MP: 150 °C; IR (KBr): 3100–3400 (NHs, OH), 1660, 1681 (C=O), 1450–1600 (aromatic C-H); ^{1}H-NMR (d_6-DMSO, 400 MHz) δ ppm, 4.42–4.44 (d, 2H, CH_2-N, $J = 8$ Hz), 6.71–6.73 (d, 2H, 4-hydroxyphenyl H_3/H_5, $J = 8$ Hz), 7.21–7.24 (t, 1H, N-benzyl (*p*), $J = 8$ Hz), 7.27–7.31 (t, 2H, N-benzyl (*m*), $J = 8$ Hz), 7.35–7.37 (d, 2H, N-benzyl (*o*), $J = 8$ Hz), 7.48–7.50 (d, 2H, 4-hydroxyphenyl H_2/H_6, $J = 8$ Hz), 7.51–7.60 (m, 4H, phenylene H_2/H_3/H_4/H_5), 8.87–8.90 (t, 1H, NH, $J = 8$ Hz), 9.21 (s, 1H, OH), 10.10 (s, 1H, NH); ^{13}C-NMR (d_6-DMSO, 100 MHz) δ ppm; 42.92, 115.40, 121.74, 127.11, 127.59, 128.08, 128.22, 128.64, 129.79, 130.04, 131.72, 136.45, 137.67, 139.92, 153.85, 166.95, 168.44; LC-MS (ESI) *m/z* 345.2 (M-H$^+$); Anal. Calcd for $C_{21}H_{18}N_2O_3$: C, 72.82; H, 5.24; N, 8.09. Found: C, 72.71; H, 5.22; N, 8.11.

N^1-benzyl-N^2-(1-phenylethyl) phthalamide (3v)

Yield: 77%; MP: 193 °C; IR (KBr): 3256, 3313 (NHs), 1646, 1663 (C=O), 1450–1600 (aromatic C-H); ^{1}H-NMR (d_6-DMSO, 400 MHz) δ ppm, 1.39–1.41 (d, 3H, CH_3, $J = 8$ Hz), 4.40–4.42 (d, 2H, CH_2-N, $J = 8$ Hz), 5.07–5.10 (m, 1H, CH), 7.21–7.29 (m, 2H, N-benzyl (*p*) & phenethyl (*p*)), 7.30–7.37 (m, 6H, N-benzyl (*o*, *m*) & phenetyhl (*m*)), 7.41–7.42 (d, 2H, phenethyl (*o*), $J = 4$ Hz), 7.47–7.54 (m, 4H, phenylene H_2/H_3/H_4/H_5), 8.74–8.76 (d, 1H, NH, $J = 8$ Hz), 8.78–8.81 (t, 1H, NH, $J = 8$ Hz); ^{13}C-NMR (d_6-DMSO, 100 MHz) δ ppm; 22.93, 42.93, 48.73, 126.57, 127.03, 127.17, 127.65, 128.13, 128.33, 128.70, 129.78, 129.88, 136.55, 136.92, 139.91, 145.12, 167.84, 168.65; LC-MS (ESI) *m/z* 357.3 (M-H$^+$); Anal. Calcd for $C_{23}H_{22}N_2O_2$: C, 77.07; H, 6.19; N, 7.82. Found: C, 77.23; H, 6.20; N, 7.84.

N^1-benzyl-N^2-(3, 4-dimethoxybenzyl) phthalamide (3w)

Yield: 85%; MP: 160–161 °C; IR (KBr): 3210, 3310 (NHs), 1643, 1675 (C=O), 1450–1600 (aromatic C-H); ^{1}H-NMR (d_6-DMSO, 400 MHz) δ ppm, 3.37–3.39 (d, 2H, CH_2-N, $J = 5.6$ Hz), 3.71 (s, 3H, OCH_3), 3.73 (s, 3H, OCH_3), 4.42–4.44 (d, 2H, CH_2-N, $J = 6$ Hz), 6.75–6.77 (dd, 1H, dimethoxybenzyl H_5, $J = 6.4$, 1.6 Hz), 6.86–6.88 (m, 2H, dimethoxybenzyl H_2/H_6), 7.22–7.26 (t, 1H, N-benzyl (*p*), $J = 7.2$ Hz), 7.31–7.35 (t, 2H, N-benzyl (*m*), $J = 7.6$ Hz), 7.37–7.41 (m, 3H, phenylene H_4 & N-benzyl (*o*)), 7.47–7.51 (m, 3H, phenylene H_2/H_3/H_5), 8.34–8.37 (t, 1H, NH, $J = 5.6$ Hz), 8.81–8.84 (t, 1H, NH, $J = 6$ Hz); ^{13}C-NMR (d_6-DMSO, 100 MHz) δ ppm; 41.46, 42.89, 55.80, 55.94, 112.30, 113.01, 120.93, 127.13, 127.62, 128.06, 128.14, 128.66, 129.74, 129.80, 132.47, 136.62, 137.00, 139.98, 147.62, 149.02, 168.58, 168.65; LC-MS (ESI) *m/z* 403.2 (M-H$^+$); Anal. Calcd for $C_{24}H_{24}N_2O_4$: C, 71.27; H, 5.98; N, 6.93. Found: C, 71.15; H, 6.00; N, 7.00.

N^1-benzyl-N^2-phenylphthalamide (3x)

Yield: 67%; MP: 174–175 °C; IR (KBr): 3299, 3305 (NHs), 1651, 1677 (C=O), 1450–1600 (aromatic C-H); ^{1}H-NMR (d_6-DMSO, 400 MHz) δ ppm, 4.42–4.44 (d, 2H, CH_2-N, $J = 6$ Hz), 7.20–7.40 (m, 8H, N-benzyl (*o*, *m, p*) & phenyl (*m*, *p*)), 7.53–7.64 (m, 4H, phenyl (*o*) & phenylene H_3/H_4), 7.74–7.76 (m, 2H, phenylene H_2/H_5), 8.96–8.99 (t, 1H, NH, $J = 6$ Hz), 10.51 (s, 1H, NH); ^{13}C-NMR (d_6-DMSO, 100 MHz) δ ppm; 42.95, 121.49, 127.13, 127.30, 127.58, 127.66, 128.08, 128.23, 128.65, 128.97, 130.05, 130.23, 136.26, 137.44, 138.99, 167.79, 168.11; LC-MS (ESI) *m/z* 329.1 (M-H^+); Anal. Calcd for $C_{21}H_{18}N_2O_2$: C, 76.34; H, 5.49; N, 8.48. Found: C, 76.55; H, 5.46; N, 8.49.

N^1-benzyl-N^2-(4-chlorophenyl) phthalamide (3y)

Yield: 72%; MP: 178–181 °C; IR (KBr): 3301, 3322 (NHs), 1645, 1663 (C=O), 1450–1600 (aromatic C-H); ^{1}H-NMR (d_6-DMSO, 400 MHz) δ ppm, 4.42–4.44 (d, 2H, CH_2-N, $J = 5.6$ Hz), 7.09–7.11 (t, 1H, N-benzyl (*p*), $J = 7.2$ Hz), 7.19–7.41 (m, 6H, N-benzyl (*o*, *m*) & 4-chlorophenyl H_3/H_5), 7.48–7.63 (m, 4H, 4-chlorophenyl H_2/H_6 & phenylene H_3/H_4), 7.74–7.76 (m, 2H, phenylene H_2/H_5), 8.96–8.99 (t, 1H, NH, $J = 5.6$ Hz), 10.39 (s, 1H, NH); ^{13}C-NMR (d_6-DMSO, 100 MHz) δ ppm; 45.79, 123.75, 127.11, 127.59, 128.08, 128.26, 128.64, 128.90, 129.05, 129.41, 129.93, 130.15, 134.56, 136.33, 137.63, 167.67, 168.26; LC-MS (ESI) *m/z* 363.1 (M-H^+); Anal. Calcd for $C_{21}H_{17}ClN_2O_2$: C, 69.14; H, 4.70; N, 7.68. Found: C, 69.25; H, 4.68; N, 7.71.

N^1-benzyl-N^2-((1R, 2R)-2-hydroxy-2, 3-dihydro-1H-inden-1-yl) phthalamide (3z)

Yield: 54%; MP: 174–175 °C; IR (KBr): 3299, 3305 (NHs, OH), 1651, 1677 (C=O), 1450–1600 (aromatic C-H); ^{1}H-NMR (d_6-DMSO, 400 MHz) δ ppm, 2.70–2.76 (q, 1H, aminoindanol H_3, $J = 8$ Hz), 3.10–3.16 (q, 1H, aminoindanol $H_{3'}$, $J = 8$ Hz), 4.30–4.48 (m, 3H, CH_2-N & CH-O), 5.19–5.23 (t, 1H, CH-N, $J = 8$ Hz), 5.35–5.36 (d, 1H, OH, $J = 4$ Hz), 7.15–7.57 (m, 13H, phenylene $H_2/H_3/H_4/H_5$ & aminoindanol $H_4/H_5/H_6/H_7$ & N-benzyl (*o,m, p*)), 8.67–8.70 (d, 1H, NH, $J = 12$ Hz), 8.89–8.92 (t, 1H, NH, $J = 8$ Hz); ^{13}C-NMR (d_6-DMSO, 100 MHz) δ ppm; 42.78, 46.04, 61.70, 78.08, 127.03, 127.13, 127.65, 127.93, 128.08, 128.34, 128.69, 128.89, 129.08, 129.28, 129.76, 129.82, 134.73, 136.72, 137.16, 139.94, 168.77, 169.22; LC-MS (ESI) *m/z* 385.1 (M-H^+); Anal. Calcd for $C_{24}H_{22}N_2O_3$: C, 74.59; H, 5.74; N, 7.25. Found: C, 74.45; H, 5.73; N, 7.28.

In vitro anti-HCV and cytotoxicity assays

Cell culture and virus production

Huh7.5, a Huh7 variant cell line, originated from HCC that is highly permissive to efficient HCV RNA multiplication (kindly provided by Rice C) was cultured in Dulbecco's modified Eagle's medium (DMEM) (Gibco®) supplemented with 10% fetal bovine serum (FBS), 100 U/mL of penicillin and 100 µg/mL of streptomycin [23]. The full-length HCV JFH1 genome (kindly provided by Wakita T) was used for in vitro transcription to produce approximately high-titer stocks of infectious particles in cell culture (HCVcc) as previously described [24, 25].

RT-qPCR assay

The RT-qPCR analysis was used to explore the inhibitory effects of our newly synthesized compounds. Briefly, 24 h before infection, 3×10^5 Huh7.5 cells were seeded in 48-well plates with DMEM containing 10% FBS. Then the huh7.5 cells were treated with HCV viral stock (10^5 IU/ml) for 3 h, at which point the infection was stopped. The supernatant was discarded, and each well was washed three times with phosphate buffer saline (PBS) to removed non penetrated virions. Then the fresh medium was added to each well. Subsequently, the infected cells were treated with different levels of newly-synthesized compounds as well as the sofosbuvir (Sigma–Aldrich, USA) as the standard. 72 h post-inoculation, the supernatant medium had been collected and viral RNA extracted, under the manufacturer's protocol, using the viral QIAamp viral mini kit of RNA (Qiagen, Düsseldorf, Germany). Then, the number of HCV RNA copies was measured using a quantitative RT-PCR assay by HCV Viral load kit (Gene Proof, Czech Republic, with CE, IVD) as directed by the manufacturer. The 50% inhibitory concentration (IC_{50}), which was defined as the concentration of analog at which the secreted HCV virions were decreased by 50% relative to the control reactions (infected wells in the absence of drug), was determined by nonlinear regression analysis using GraphPad Prism5.0 software (GraphPad Software, San Diego, CA).

Cytotoxicity assay

In parallel with the in vitro evaluation of anti-HCV effects, the XTT (sodium 3-[1(phenylaminocarbonyl)-3,4-tetrazolium]-bis(4-methoxy-6-nitro)benzene sulfonic acid) assay was carried out to evaluate the cytotoxicity of compounds to Huh-7.5 cells, according to XTT proliferation kit (Sigma–Aldrich) instructions [26]. In this regard, cells were

treated with various concentrations (500, 250, 100, 25, and 12 µm/ml) of newly-synthesized analogs and incubated for 72 h. Then, the amount of orange formazan dye generated via the cleavage of the yellow tetrazolium salt XTT by the viable cells was measured using the UV-visible spectrophotometry method [27].

Docking studies

The protein structure was prepared for docking by the use of AutoDockTools® [28]. The docking analysis was performed using Autodock VINA® operating system [29]. Molecules were built within chemdraw® and subsequently optimized using the Hyperchem 8.0 software. The 3D protein structure of the HCV polymerase enzyme with its cognate ligand, UTP (PDB code: 1GX6), was downloaded from the Protein Data Bank of the Research Collaboration for Structural Bioinformatics (RCSB) website [30]. Co-crystallized ligand and water molecules were removed from the protein structure, while Mn^{2+} ions remained intact. The receptors and ligands were treated as rigid and flexible structures, respectively. Non-polar hydrogens were merged. Polar hydrogens and Kollman united partial atom charges were added to the individual protein atoms. The grid box that was set around the amino acids involved in the binding site, had the dimension of $60 \times 60 \times 60$ ($x \times y \times z$) along with a centroid at $x = 14.14$, $y = 24.58$, and $z = 30.65$. Docking results were clustered with a root mean square deviation (RMSD) of 0.5 Å and evaluated by Pymol software version 1.5.0.1. moreover, the surface presentation of the active site and **3z** was applied to clear the interaction of the ligand-protein.

Funding This work was supported by a grant from the Research Council of Shaheed Beheshti University of Medical Sciences [30030].

Compliance with ethical standards

Conflict of interest The authors declare no competing interests.

References

1. Axley P, Ahmed Z, Ravi S, Singal AK. Hepatitis C virus and hepatocellular carcinoma: a narrative review. J Clin Transl Hepatol. 2018;6(1):79.
2. Zoulim F, Liang TJ, Gerbes AL, Aghemo A, Deuffic-Burban S, Dusheiko G, et al. Hepatitis C virus treatment in the real world: optimising treatment and access to therapies. Gut. 2015;64(11): 1824–33.
3. Jefferies M, Rauff B, Rashid H, Lam T, Rafiq S. Update on global epidemiology of viral hepatitis and preventive strategies. World J Clin Cases. 2018;6(13):589–99.
4. Palumbo E. Pegylated interferon and ribavirin treatment for hepatitis C virus infection. Ther Adv Chronic Dis. 2011;2(1):39–45.
5. Manns MP, Wedemeyer H, Cornberg M. Treating viral hepatitis C: efficacy, side effects, and complications. Gut. 2006;55(9):1350–9.
6. Abdelwahab KS, Ahmed Said ZN. Status of hepatitis C virus vaccination: Recent update. World J Gastroenterol. 2016;22(2):862–73.
7. Gupta V, Kumar A, Sharma P, Arora A. Newer direct-acting antivirals for hepatitis C virus infection: Perspectives for India. Indian J Med Res. 2017;146(1):23–33.
8. Alazard-Dany N, Denolly S, Boson B, Cosset F-L. Overview of HCV Life Cycle with a Special Focus on Current and Possible Future Antiviral Targets. Viruses. 2019;11(1):30.
9. Kumthip K, Maneekarn N. The role of HCV proteins on treatment outcomes. Virol J. 2015;12:217.
10. Rabbani SMIM, Vahabpour R, Hajimahdi Z, Zarghi A. Design, Synthesis, Molecular Modeling Studies and Biological Evaluation of N′-Arylidene-6-(benzyloxy)-4-oxo-1, 4-dihydroquinoline-3-carbohydrazide Derivatives as Novel Anti-HCV Agents. Iran J Pharm Res. 2019;18(4):1790.
11. Powdrill MH, Bernatchez JA, Götte M. Inhibitors of the Hepatitis C Virus RNA-Dependent RNA Polymerase NS5B. Viruses. 2010;2(10):2169–95.
12. Appleby TC, Perry JK, Murakami E, Barauskas O, Feng J, Cho A, et al. Structural basis for RNA replication by the hepatitis C virus polymerase. Science. 2015;347(6223):771–5.
13. Ng KKS, Arnold JJ, Cameron CE. Structure-function relationships among RNA-dependent RNA polymerases. Curr Top Microbiol Immunol. 2008;320:137–56.
14. Bhatt A, Gurukumar KR, Basu A, Patel MR, Kaushik-Basu N, Talele TT. Synthesis and SAR optimization of diketo acid pharmacophore for HCV NS5B polymerase inhibition. Eur J Med Chem. 2011;46(10):5138–45.
15. Deng Y, Shipps GW Jr, Wang T, Popovici-Muller J, Rosner KE, Siddiqui MA, et al. Discovery of 4Hpyrazolo [1, 5-a] pyrimidin-7-ones as potent inhibitors of hepatitis C virus polymerase. Bioorg Med Chem Lett. 2009;19(18):5363–7.
16. Venkatraman S, Velazquez F, Gavalas S, Wu W, Chen KX, Nair AG, et al. Discovery of novel tricyclic indole derived inhibitors of HCV NS5B RNA dependent RNA polymerase. Bioorg Med Chem. 2013;21(7):2007–17.
17. Zhao C, Wang Y, Ma S. Recent advances on the synthesis of hepatitis C virus NS5B RNA-dependent RNA-polymerase inhibitors. Eur J Med Chem. 2015;102:188–214.
18. Sena VL, Srivastava RM, Oliveira SP, Lima VL. Microwave assisted synthesis of N-Arylphthalamic acids with hyperlipidemic activity. Bioorg Med Chem Lett. 2001;11(20):2671–4.
19. Higuchi T, Miki T, Shah AC, Herd AK. Facilitated Reversible Formation of Amides from Carboxylic Acids in Aqueous Solutions. Intermediate Production of Acid Anhydride. J Am Chem Soc. 1963;85(22):3655–60.
20. Smith SN, Connon SJ. Preparation of Lactams from Cyclic Anhydrides via N-Carboxyanhydride Intermediates. Eur J Org Chem. 2021;2021(40):5540–4.
21. Lohmann V, Körner F, Koch J-O, Herian U, Theilmann L, Bartenschlager R. Replication of subgenomic hepatitis C virus RNAs in a hepatoma cell line. Science. 1999;285(5424):110–3.
22. Blight KJ, Kolykhalov AA, Rice CM. Efficient initiation of HCV RNA replication in cell culture. Science. 2000;290(5498):1972–4.
23. Cai Z, Liang TJ, Luo G. Effects of mutations of the initiation nucleotides on hepatitis C virus RNA replication in the cell. J Virol. 2004;78(7):3633–43.
24. Wakita T, Pietschmann T, Kato T, Date T, Miyamoto M, Zhao Z, et al. Production of infectious hepatitis C virus in tissue culture from a cloned viral genome. Nat Med. 2005;11(7):791–6.
25. Mateu G, Donis RO, Wakita T, Bukh J, Grakoui A. Intragenotypic JFH1 based recombinant hepatitis C virus produces high levels of infectious particles but causes increased cell death. Virology 2008;376(2):397–407.

26. Scudiero DA, Shoemaker RH, Paull KD, Monks A, Tierney S, Nofziger TH, et al. Evaluation of a soluble tetrazolium/formazan assay for cell growth and drug sensitivity in culture using human and other tumor cell lines. Cancer Res. 1988;48(17):4827–33.
27. Stockert JC, Horobin RW, Colombo LL, Blázquez-Castro A. Tetrazolium salts and formazan products in Cell Biology: Viability assessment, fluorescence imaging, and labeling perspectives. Acta Histochem. 2018;120(3):159–67.
28. Morris GM, Goodsell DS, Halliday RS, Huey R, Hart WE, Belew RK, et al. Automated docking using a Lamarckian genetic algorithm and an empirical binding free energy function. J Comput Chem. 1998;19(14):1639–62.
29. Trott O, Olson AJ. AutoDock Vina: improving the speed and accuracy of docking with a new scoring function, efficient optimization, and multithreading. J Comput Chem. 2010;31(2):455–61.
30. Bressanelli S, Tomei L, Rey FA, De Francesco R. Structural analysis of the hepatitis C virus RNA polymerase in complex with ribonucleotides. J Virol. 2002;76(7):3482–92.

Publisher's note Springer Nature remains neutral with regard to jurisdictional claims in published maps and institutional affiliations.

Springer Nature or its licensor holds exclusive rights to this article under a publishing agreement with the author(s) or other rightsholder(s); author self-archiving of the accepted manuscript version of this article is solely governed by the terms of such publishing agreement and applicable law.